Graphene Translucency and Interfacial Interactions in the Gold/Graphene/SiC System

Mario Caccia,[1] Donatella Giuranno,[2] José M. Molina-Jorda,[1] Mónica Moral,[3] Rafal Nowak,[4] Enrica Ricci,[2] Natalie Sobczak,[4] Javier Narciso,[1] Javier Fernández Sanz[3]*

[1]*Departamento de Química Inorgánica e Instituto Universitario de Materiales de Alicante, Universidad de Alicante, Alicante (Spain)*

[2] *National Research Council (CNR), Institute of Condensed Matter Chemistry and Energy Technologies (ICMATE), Genoa (Italy)*

[3]*Departamento de Química Física, Universidad de Sevilla, Sevilla (Spain)*

[4]*Foundry Research Institute, Krakow (Poland)*

Abstract

Integration of graphene into electronic circuits through its joining with conventional metal electrodes (i.e. gold) appears to be one of the main technological challenges nowadays. To gain insight into this junction, we have studied the physicochemical interactions between SiC-supported graphene and a drop of molten gold. Using appropriate high temperature experimental conditions we perform wetting experiments and determine contact angles for gold drops supported on graphene epitaxially grown on 4H-SiC. The properties of the metal/graphene interface are analyzed using a wide variety of characterization techniques, along with computational simulations based on density functional theory. In contrast with the established, our outcomes clearly show that graphene is translucent in the SiC-graphene-gold interface and therefore its integration into electronic circuits primarily depends on the right choice of the support to produce favorable wetting interactions with liquid gold.

TOC Graphic

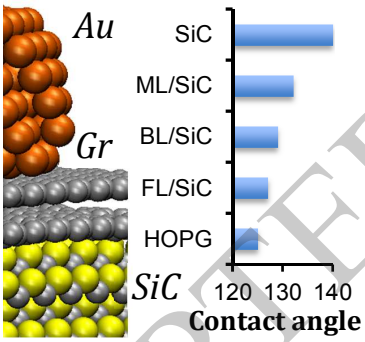

Graphene characterizes by its peculiar structure of a single-atom-thick sheet of sp^2-hybridized carbon atoms arranged in a hexagonal honeycomb lattice. It displays a unique combination of properties: it is flexible, chemically stable, mechanically strong, and exhibits a high electrical and thermal conductivity, along with a tunable band gap. It is also optically transparent at 90%.[1] These properties open the possibility for the electronics industry to fabricate next generation ultra-fast electronic components. Recently, it was reported that SiC-based field emission transistors (FETs) exhibit higher mobility than classical Si-based transistors[2] and that their performance could be further improved by adding a graphene layer to the SiC wafer.[3] Since the process of epitaxial growth of graphene on SiC by Si atoms sublimation is nowadays well-known and controlled, it would be easy to integrate both materials to microelectronic components. Furthermore, the ability to control the conductive behavior of epitaxially grown graphene on SiC opens a window of opportunity for this novel material. However, the integration of graphene into electronics components by classical liquid-assisted joining techniques seems to be the main technological challenge. Research on physicochemical interactions of graphene and liquid metals seems mandatory in order to assess the integration of graphene in electronic circuits and components.

On the other side, recent researches[4] have deepened in the interfacial interactions of graphene and liquid water, especially reporting its wetting behavior. In this line, various studies[5] concluded that it is possible to independently tune the properties of surfaces without disrupting their wetting response, except for super-hydrophobic and super-hydrophilic substrates, for which wetting transparency breaks down significantly. The wetting transparency of graphene towards water motivates the study of other liquids with intrinsic importance in electronics, like conventional metals used for joining (e.g. gold). The recently called wetting transparency of graphene towards water has created a great controversy, as some authors comment that the experiments were not properly conducted since the chemistry of the surface of graphene is modified by being exposed to the environment, as it happens to any carbon material, greatly modifying its wetting properties.[6] As a consequence, in order to obtain high quality data, there is a need to establish an experimental protocol with a very thorough control of the operative conditions and procedures as well as the properties and quality of substrate.

In the present work, we present, for the first time, a thorough study on the physicochemical interactions between epitaxial graphene grown on 4H-SiC and liquid gold. To assess these interactions two complementary approaches have been used. The

macroscopic wetting behavior of the system was studied experimentally using the sessile drop technique by depositing liquid gold on SiC-supported graphene at 1373 K under ultra-clean conditions. In order to understand the fundamental phenomena involved in the interactions between the liquid and the substrate, and to explain the wetting responses observed, a computational analysis of the interaction energies between epitaxial graphene on SiC and gold, based on first-principles periodic Density Functional Theory (DFT) calculations, was performed. In both cases we employed SiC-supported graphene with variable thickness (from 1 to more than three graphene layers). We conclude that the interaction between gold and SiC does get partially transmitted through the graphene layer, being the system less translucent as the number of graphene sheets is augmented. Integration of graphene as a key element in electronics is then proved to be strongly dependent on the right choice of the support within which the liquid gold should establish favorable wetting interactions.

The experimental study used large-area (7x7 mm^2) substrates of epitaxial graphene of variable thickness, grown on 4H-SiC. The number of graphene layers (N) was varied from N=1 (ML) to N=3-4(FL). **Figure 1** shows the Raman spectra and the Scanning Probe Microscope (SPM) 2D-topography of the substrates used. The intensity ratio between the 2D band and the G band were found to be consistent with the number of layers in the different substrates, and the SPM measurements showed homogeneous coating over the smooth SiC surface. A more detailed description of the characterization of the substrates before and after the experiments is provided in the Supporting Information.

a) b)

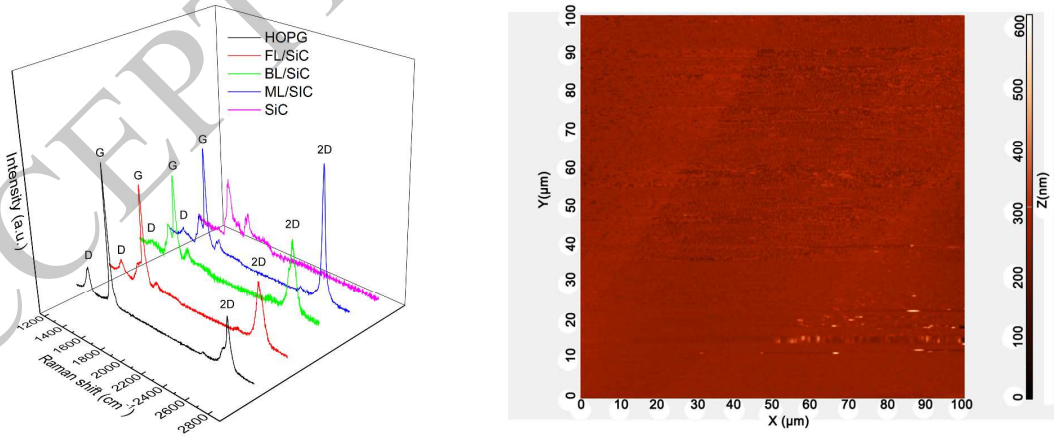

Figure 1. a) Raman spectra of the substrates, and b) a representative SPM 2D-topography image of the surface of the ML/SiC substrate.

Unlike in transported graphene, in epitaxially grown graphene there is a buffer layer between the SiC substrate and the first graphene monolayer (see **Figure 2**). This layer is the result of a surface reconstruction after Si atom sublimation and exhibits a mixed hybridized sp^3+sp^2 structure.[7] Even though the buffer layer is composed exclusively of carbon atoms, it does not possess the properties of graphene, and it only acts as an interface between graphene and SiC.

The nomenclature followed for the samples was SiC_{free} for SiC bare structure; SiC for the SiC+C buffer, HOPG for the highly oriented pyrolytic graphite and ML/SiC, BL/SiC, FL/SiC for silicon carbide-supported graphene consisting of one, two and few (between 3-4), graphene layers, respectively. Both experimental and theoretical studies demonstrate that the presence of graphene on a SiC substrate, acts as a translucent barrier for the interactions between the SiC substrate and the pure metal. Right ahead, both borderline cases of study are detailed.

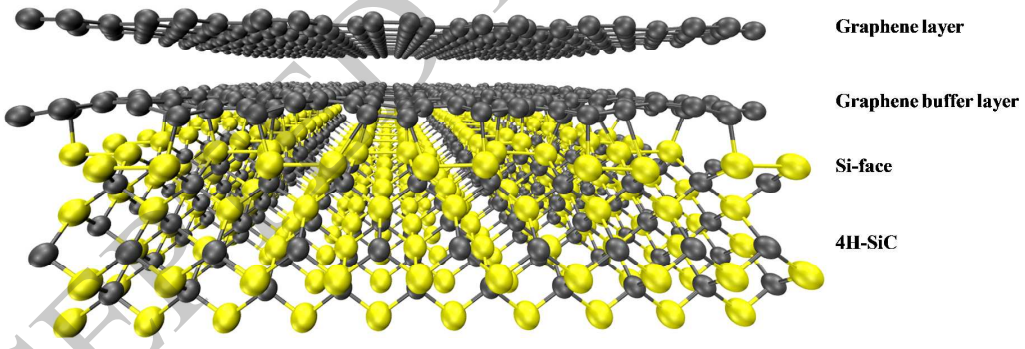

Figure 2. Scheme of the structure of epitaxial monolayer graphene on a SiC substrate.

The wetting experiments were performed at a temperature of T_{exp}= 1373 K by a sessile drop method under ultra-clean conditions both under dynamic vacuum (p~10^{-5} Pa at RT and p ~ 10^{-3} Pa at T_{exp}) and under flowing Ar (N5.0 p ~ $9 \cdot 10^4$ Pa). Heating rate up to T_{exp} was 12 K/min while after wettability test the drop/substrate couple was cooled at a rate of 2

K/min. The details of wettability tests are given in the Supporting Information. The results of contact angle of liquid gold on different substrates are collected in **Figure 3**.

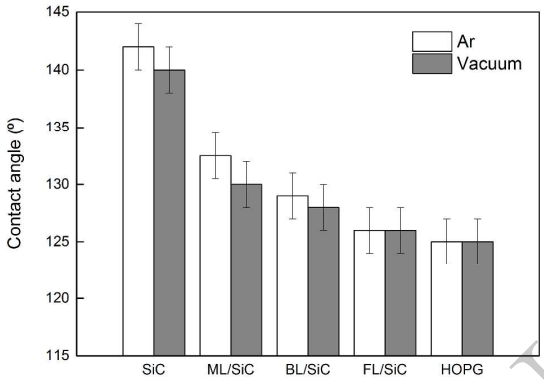

Figure 3. Measured contact angles for liquid Au on different substrates. The error bars represent the experimental measurement error.

The contact angles values measured under vacuum are slightly lower than those obtained under Ar atmosphere. This result is explained by the characterization with Raman spectroscopy (see Supporting Information) that shows that graphene layers are growing during experiments under vacuum at T_{exp}. Contact angles measured under Ar atmosphere showed decreasing values for increasing numbers of graphene layers. The same trend with the number of graphene layers is observed for contact angles obtained under vacuum. For ease, the results obtained under Ar atmosphere will be herein commented.

The contact angle of Au on carbon was found to be dependent on the crystallinity of the carbon substrate.[8] On monocrystalline graphite, the contact angle at 1373 K was reported to be 119º, and on vitreous carbon, a value of 135º was reported.[8] In the present experiments, the contact angle value of gold on HOPG was found to be 125º. This value falls in the narrow range between the two literature values, closer to the value corresponding to a perfectly monocrystalline surface given the highly oriented graphitic basal planes characteristic of the HOPG material. As aforementioned, the wettability of carbon materials is highly influenced by the surface chemistry of the substrate.[8] In this work, to ensure the cleanest surface possible, both uncoated substrates (HOPG and SiC) were previously etched using an ion beam gun and as that, directly transported through the experimental complex into the working chamber, under high vacuum conditions.[9]

In both series of experiments, the contact angle is larger for SiC than for HOPG, showing a smooth lowering as the number of graphene layer is increased (from left to right in **Figure 3**). For the FL/SiC material the contact angle is 127º, which is increased to 129º when two graphene layers are present (BL/SiC) and to 132º when only a monolayer is supported on the SiC substrate (ML/SiC). The contact angle value of liquid gold on SiC here obtained is approximately 140º. The values found in the literature for the Au/SiC system fall in the range of 120-140º. However, it was stated by Eustathopoulos *et al*. that those values were actually not representative of a contact between Au and SiC but rather of an Au-C-SiC contact, as SiC seems to be always covered with a thin graphite layer that strongly affects both the wetting behavior and the reaction kinetics.[10] In our experiments, no reactivity between Au and monocrystalline SiC was observed after 30 min at 1373 K, despite the fact that Drevet *et al.* have reported that Au may attack SiC, estimating a Si concentration in Au of $X_{Si}=10^{-6}$ after 30 min at 1373 K.[11] Different characterization techniques were performed after wetting experiments (see Supplementary Information) aimed at checking i) the composition of the metal after solidification and ii) the integrity of graphene below the droplet of solidified gold. By EDX analysis and Raman spectroscopy, no traces of other elements in the metal were found, thereby ensuring that the interaction between liquid gold/graphene/SiC substrate does not involve dissolution into the metal of either silicon or carbon from the SiC. This is further supported by the fact that the value of contact angle during each experiment remains constant after 30 min of isothermal conditions. Graphene integrity after wetting experiments was demonstrated by post-mortem Raman spectroscopy analysis.

In view of the results obtained in the present work, summarized in **Figure 3**, it becomes clear that graphene acts as a translucent barrier for the interactions between the SiC support and the liquid gold at 1373 K.

The interaction between gold and graphene was analyzed from a theoretical point of view through periodic-DFT calculations including dispersion corrections. The general model consists of a gold nanoparticle (NP) of 140 atoms deposited on several surface models intended to represent the different scenarios considered in the experimental work. The Au/surface contact is done through a face of the Au nanocrystal exposing 18 atoms. The simplest model consists of the Au_{140} NP deposited on a perfect sheet of graphene, hereafter labeled as ML (see **Figure 4a**). The Au_{140} NP may also be deposited on a bilayer of graphene, BL (see **Figure 4b**), and on a multilayer of graphene to mimic highly oriented pyrolytic graphite, HOPG (see **Figure 4c**). To represent the free SiC surface we used a nine-

atomic layer slab with a Si termination (see **Figure 4d**). This surface, SiC_{free}, might be topped by a one-layer sheet of graphene, which acts as buffer (model SiC, see **Figure 4e**), or by a graphene monolayer, supported over the previous SiC+C buffer model (model ML/SiC, see **Figure 4f**). Optimized geometric structures of these models are reported in **Figure 4**.

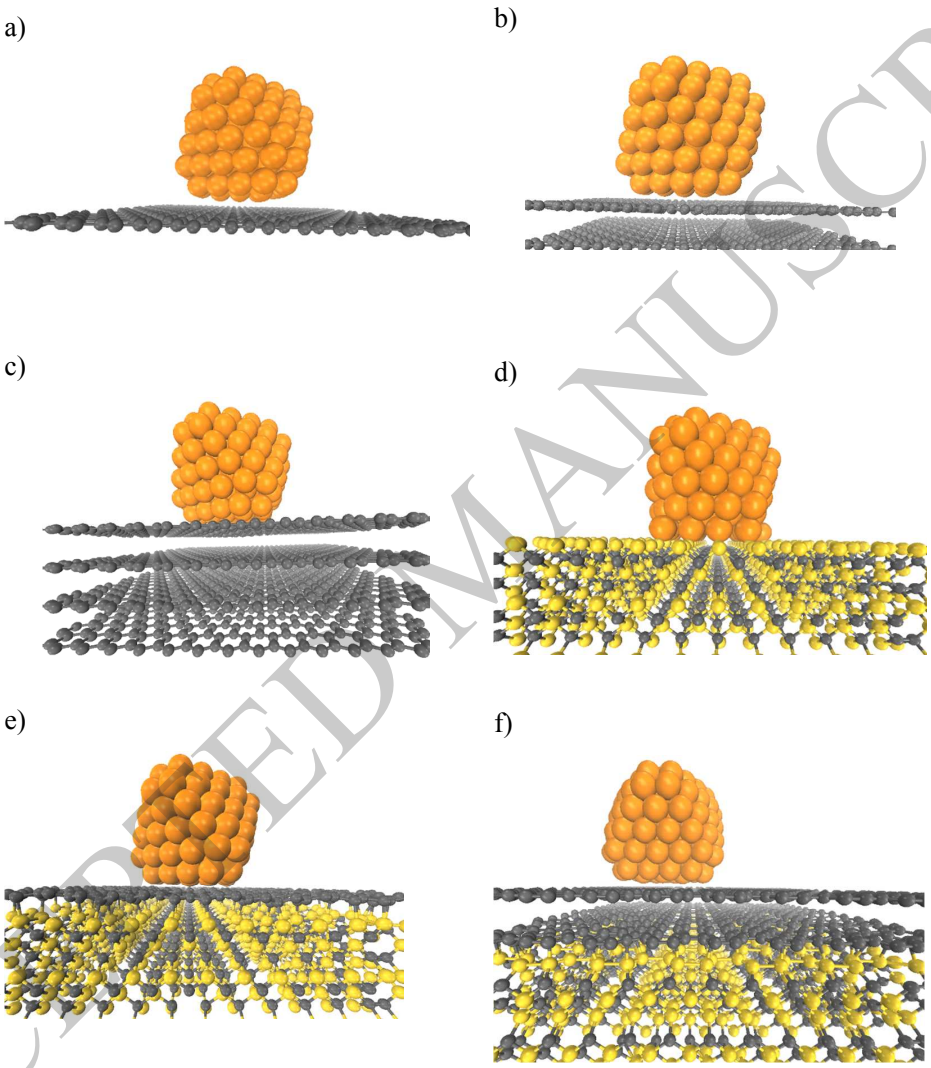

Figure 4. Optimized geometries for the Au_{140} NP deposited on a) ML; b) BL; c) HOPG; d) SiC_{free}; e) SiC; f) ML/SiC model surfaces.

The surfaces were represented by means of the supercell approach using an orthorhombic cell that is replicated into the three directions. The parameters of the supercell were a = 30.5 Å and b = 30.5 Å. These values were determined to minimize the mismatch

between graphene and SiC (0001) surfaces and are large enough to neglect lateral interaction between Au NPs. In the *c* direction, the length of the supercell is kept to 50 Å, which allows for a suitable vacuum between slabs. The atomic composition for the different supercell models is: ML: C_{336}; BL: C_{672}; HOPG: C_{1344}; SiC_{free}: $Si_{500}C_{400}$; SiC: $Si_{500}C_{736}$: ML/SiC: $Si_{500}C_{1072}$. As a first check of the surface models, the optimized structure for SiC_{free} was found to agree with the studies reported by Qi *et al.*[11] The distance between SiC outer plane and the one-layer sheet of graphene topping the surface, was also found in agreement with the results obtained by de Lima *et al.*[12] It is worth noting that the thermodynamic studies reported by Eustathopoulos *et al.*[8] showed that in the interaction between Au and SiC_{free} surface, the bonding between Si and Au is an order of magnitude higher than between gold and carbon. This behavior agrees with the theoretical findings presented here.

Table 1 shows the values for the adsorption energies obtained after the Au_{140} nanoparticle is deposited (and optimized) on the model surfaces. The highest adsorption energy per atom, 265.3 kJ/mol, has been obtained for the SiC_{free}+Au_{140} system, which is consistent with the presence of a covalent interaction between Si and Au atoms (see **Figure 1**). The Si-Au bond lengths fall in the 2.37 – 2.42 Å range, close to the values for Si-Au bonds found in Au clusters supported over Si (111).[13] The averaged distance between the top Si plane and the bottom Au layer is of 1.7 Å.

Table 1. Adsorption energies (E_{ads} by interfacial Au atom, in kJ/mol) for the Au_{140} nanoparticle deposited on different model surfaces. $D_{surf\text{-}Au}$ refers to the averaged distance (in Å) between the top surface layer and the bottom Au layer.

	SiC_{free}	ML	BL	HOPG	SiC	ML/SiC
E_{ads}	265.3	20.9	21.8	28.5	43.1	26.8
$D_{surf\text{-}Au}$	1.7	3.3	2.8	2.6	2.3	2.7

In the case of the graphene (ML and BL) and graphite (HOPG) structures, the computed adsorption energies per atom were found to be much lower, with values close each other: 20.9, 21.8 and 28.5 kJ/mol, respectively. The averaged distances between the top plane of carbon atoms and the bottom layer of Au atoms in these structures are of 3.2, 2.8 and 2.6 Å for ML, BL and HOPG, respectively, indicating that for these models the Au-NP/surface interaction is ruled by Van der Waals forces. Let us now consider the graphene-intercalated models. The adsorption energies estimated for SiC+Au_{140} is 43.1 kJ/mol, i.e. practically twice

that computed for ML model, however, it still is significantly lower that found for the bare SiC free surface. The C-Au bond lengths are ranging from 2.26 Å to 2.55 Å, which are too far from the typical C-Au bond length.[14] The surface/Au-NP interlayer average distance is of 2.3 Å. In the case of ML/SiC model surface, a further lowering in the adsorption energy is observed, 26.8 kJ/mol. This value is close to that found for HOPG or even BL, indicating that the interactions introduced by the SiC surface are almost damped. A similar conclusion might be obtained from the surface/Au-NP interlayer average distance that now amounts for 2.7 Å.

In consequence, the analysis of the adsorption energies reveals that the strong interaction between SiC_{free} and Au NPs surfaces is partially shielded by the intercalated graphene sheets. In terms of wettability of the system, these findings indicate that graphene layer/s should be considered as being translucent with respect to the Au/SiC_{free} interaction.

To summarize, we have shown that if we take as reference carbon buffered silicon carbide surfaces (model 4e), the growth of epitaxial graphene layers (model 4f) does not significantly disrupt the wetting behavior of liquid gold onto such SiC substrates. Precise contact angle measurements at 1373 K and theoretical calculations allow us to conclude that the translucency of graphene depends on the numbers of constituent layers, being a graphene monolayer 70% translucent while a three-layer graphene is only 30%. Furthermore, we demonstrate that graphene remains structurally unaltered below the liquid gold, thus guarantying an excellent electronic contact between substrate and metal. Within this scenario, the integration of substrate-supported graphene into electronic circuits, in order to take advantage of its superior electron transport properties, seems dominated by the choice of a proper substrate able to efficiently establish long-range interactions with gold trough a few-layered graphene coating.

SUBSTRATE ANALYSIS

*** Prior to wetting tests**

Before wetting tests, the surface of each substrate was characterized by means of Raman spectroscopy using a He laser (633 nm). Moreover, Auger spectroscopy was used as an alternative method to determine the number of graphene layers. XPS was also used in order to study the surface chemistry and bonding of the different materials conforming the substrates for wetting experiments. Results from these characterizations are collected in the Supplementary Information section.

*** During wetting tests**

Mass spectroscopy analysis allowed identify the different chemical species that got desorbed during the first stage of heating in wetting test (until 973 K) for the different SiC-supported graphene substrates. Results are shown in the Supplementary Information section.

*** Post-wetting tests**

After wetting experiments, the surface of the substrates surrounding the drop of Au, and the surface below the drop were analyzed using Raman spectroscopy to evaluate the structural changes in graphene. To ensure a complete removal of metal on the substrate the solidified droplet was eliminated by dissolution into mercury, in a special in-house made device that ensures no contact between substrate and mercury (Figure S1 in Supplementary Information). Results are shown in the Supplementary Information section.

CONTACT ANGLE MEASUREMENTS

The wetting experiments were performed under very clean conditions created by turbomolecular and ionic pumps and tantalum heater in an experimental complex for investigations of high-temperature capillarity phenomena (*9*) located at the Center for High Temperature Studies of Liquid Metals and Alloys of the Foundry Research Institute, Cracow. This equipment integrates several unique features in the sessile drop wettability test equipment. It can work at temperatures up to 2300 K and a vacuum up to 10^{-5} Pa or under protective atmosphere (static or flowing gas with controlled rate at a required level of pressure). During the wettability tests, the images of drop/substrate couples were recorded by means of high-speed high-resolution camera MC1310 with a rate of 100 frames per second (fps). The collected images were used for estimation of the contact angle values with dedicated software developed by CNR-ICMATE Italy).

THEORETICAL CALCULATIONS

Periodic DFT calculations have been performed using the VASP.[15,16] The Projector Augmented Wave (PAW) method has been used to represent atomic cores effect on the valence electron density.[17,18] The generalized gradient approximation (GGA) was adopted to describe the electron-electron exchange and correlation interactions, by employing the Perdew, Burke and Ernzherhof (PBE) functional.[19] The PBE functional has been proven to adequately reproduce the experimental data for both graphene and transition metals.[20] The electronic one-particle wave functions were expanded in a plane wave basis set up to an energy cut-off of 300 eV. Gradients and energies were computed at the gamma point. In the geometry minimizations, all atoms were allowed to relax, stopping the optimization when changes in energy where smaller than 0.001 eV, which in general means that all forces acting on atoms became less than 0.02 eV $Å^{-1}$.

It is well known that dispersion forces dominate the interaction between gold surfaces and for instance, aromatic molecules. For this reason, the calculations were carried out including the semi-empirical DFT-D2 dispersive correction developed by Grimme.[21] The values of dispersion coefficient (C_6) and Van der Waals radius (R_0) for C and Si were those originally proposed by Grimme in the original discussion of his method,[21] while for gold we used the parameters proposed by Nguyen *et al.*,[22] namely, C_6 = 21.23 J nm^6/mol and R_0 = 1.66 Å. This set of values is also close to that proposed by other authors.[23] The global scaling factor s_6, and the cut-off radius for pair interactions employed in the dispersion corrections were set to 0.75 and 30 Å respectively. To test the performance of the DFT-D2 approach in rendering the graphite structure we first determined the lattice parameters and compared them with experimental data: a = 2.46 Å and c = 6.71 Å.[24] Plain PBE calculations give a = 2.47 Å, in agreement with experiment, while the value of c = 7.98 Å is overestimated by 1.27 Å, clearly illustrating that interactions between carbon layers are mostly neglected. Including the dispersion forces through the DFT-D2 approach dramatically improves the description giving values in good agreement with the experimental data: a = 2.46 Å and c = 6.43 Å.

The absorption energy, E_{ads}, were calculated by the following equation

$$E_{ads} = (E_{surf} + E_{AuNP}) - E_{surf/AuNP} \qquad (1)$$

where $E_{surf/AuNP}$, E_{surf} and E_{AuNP} correspond with the total energy of the relaxed adsorption complex (composed by surface and Au_{140} NP), the energy of the clean surface (in that case, it could be SiC_{free}, SiC+C, ML/SiC, ML, BL or HOPG) and the energy of the isolated gold NP, respectively. According to this definition, adsorption energies are defined positive, and

hence, the larger the Eads value, the stronger the interaction between the surface and the Au NP.

ASSOCIATED CONTENT

Supporting Information.

The file assembles details on the wetting tests and experimental procedures used in the measure of contact angles as well as the different characterization techniques employed to analyze the substrates before and after the experimental measures, in particular Raman and XPS/Auger spectra.

AUTHOR INFORMATION

Corresponding Author

Javier Fernández Sanz: sanz@us.es

Author Contributions

The manuscript was carried out and written through contributions of all authors. All authors have given approval to the final version of the manuscript.

ACKNOWLEDGMENTS

The work performed at the University of Alicante was funded by the Spanish "Ministerio de Economía, Industria y Competitividad" (grant MAT2016-77742-C2-2-P) and the "Generalitat Valenciana" (PROMETEO II/2014/004-FEDER). The work performed at the University of Sevilla was funded by the Spanish "Ministerio de Economía y Competitividad" (grant CTQ2015-64669-P), "Junta de Andalucía" and European FEDER (grant P12-FQM-1595). Also, Mónica Moral thanks to the E2TP CYTEMA-Santander Program for their financial support. The work performed at the Foundry Research Institute was funded by the Ministry of Science and Higher Education of Poland (Project No. IOd-6619/00). The ICMATE authors are grateful to Dr. A. Passerone for his contribution during many fruitful discussions and his suggestions on how to correctly measure and interpret contact angle values. The authors acknowledge Marta Homa and Rada Novakovic for a critical reading.

REFERENCES

1. Novoselov, K.S.; Fal, V.I.; Colombo, L.; Gellert, P.R.; Schwab, M.G.; Kim, K. A Roadmap for Graphene. *Nature* **2012**, *490*, 192–200.

2. Bhatnagar, M.; Baliga, B.J. Comparison of 6H-SiC, 3C-SiC, and Si for power devices. *IEE Transaction on Electron Devices* **1993**, *40*, 645–655.

3. Gong, G.; Shu, N.; Feenstra, R.M.; Devaty, R.P.; Choyke, W.J.; Chan, W.K.; Kane, G. Field Effect in Epitaxial Graphene on Silicon Carbide Substrate. *Appl. Phys. Lett*. **2007**, *90*, 253507.

4. Rafiee, J.; Mi, X.; Gullapalli, H.; Thomas, A.V.; Yavari, F.; Shi, Y.; Ajayan, P.M.; Koratkar, N.A. Wetting Transparency of Graphene. *Nat. Mater.* **2012**, *11*, 217–222.

5. Shih, C.J.; Strano, M.S.; Blankschtein, D. Wetting Translucency of Graphene. *Nat. Mater.* **2013**, *12*, 866–869.

6. Shih, C.J.; Wang, Q.H.; Lin, S.; Park, K.C.; Jin, Z.; Strano, M.S.; Blankschtein, D. Breakdown in the Wetting Transparency of Graphene. *Phys. Rev. Lett.* **2012**, *109*, 1–5.

7. Golera, S.; Colettia, C.; Piazza, V.; Pingue, P.; Colangelo, F.; Pellegrini, V.; Emtsev, K.V.; Fortic, S.; Starkec, U.; Beltrama, F.; Heunb, S. Revealing the Atomic Structure of the Buffer Layer Between SiC (0001) and Epitaxial Graphene. *Carbon* **2013**, *51*, 249–254.

8. Eustathopoulos, N.; Nicholas, M.G.; Drevet, B. (Eds.) Wettability at High Temperatures (Vol. 3). Elsevier Science Ltd.: Oxford, 1999.

9. Sobczak, N.; Nowak, R.; Radziwill, W.; Budzioch, J.; Glenz, A. Experimental Complex for Investigations of High Temperature Capillarity Phenomena. *Mater. Sci. Eng. A* **2008**, *495*, 43–49.

10. Drevet, B.; Kalogeropoulou, S.; Eustathopoulos, N. Wettability and Interfacial Bonding in Au-Si/SiC System. *Acta Metall. Mater.* **1993**, *41*, 3119–3126.

11. Qi, Y.; Rhim, S.H.; Sun, G.F.; Weinert, M.; Li, L. Epitaxial Graphene on SiC (0001): More than Just Honeycombs. *Phys. Rev. Lett.* **2010**, *105*, 085502.

12. De Lima, L.H.; Handschak, D.; Schönbohm, F.; Landers, R.; Westphal, C.; De Siervo. A. The Atomic Structure of a Bare Buffer Layer on SiC (0001) Chemically Resolved. *Chem. Commun.* **2014**, *50*, 13571–13574.

13. Granatier, J.; Lazar, P.; Otyepka, M.; Hobza. P. The Nature of the Binding of Au, Ag, and Pd to Benzene, Coronene, and Graphene: From Benchmark CCSD(T) Calculations to Plane-Wave DFT Calculations. *J. Chem. Theory Comput.* **2011**, *7*, 3743–3755.

14. Liu, H.T.; Xiong, X.G.; Dau. P.D.; Wang, Y.L.; Huang, D.L.; Li, J.; Wang, L.S. Probing the Nature of Gold–Carbon Bonding in Gold–Alkynyl Complexes. *Nature Commun.* **2013**, *4*,

2223.

15. Kresee, G.; Furthmüller, J. Efficient Iterative Schemes for *Ab Initio* Total-Energy Calculations Using a Plane-Wave Basis Set. *Phys. Rev. B* **1996**, *54*, 11169.

16. Kresee, G.; Furthmüller, J. Efficiency of Ab-Initio Total Energy Calculations for Metals and Semiconductors Using a Plane-Wave Basis Set. *Comput. Mater. Sci.* **1996**, *6,* 15–20.

17. Blöchl, P.E. Projector Augmented-Wave Method. *Phys. Rev. B* **1994**, *50*, 17953.

18. Kresse, G.; Jourbert, J. From Ultrasoft Pseudopotentials to the Projector Augmented-Wave Method. *Phys. Rev. B* **1999**, *59*, 1758.

19. Perdew, J.P.; Burke, K.; Ernzerhof, M. Generalized Gradient Approximation Made Simple. *Phys. Rev. Lett.* **1996**, *77*, 3865.

20. Janthon, P.; Viñes, F.; Kozlov, S.M.; Limtrakul, J.; Illas, F. Theoretical Assessment of Graphene-Metal Contacts. *J. Chem. Phys.* **2013**, *138*, 244701.

21. Grimme, S. Semiempirical GGA-Type Density Functional Constructed with a Long-Range Dispersion Correction. *J. Comput. Chem.* **2006**, *27*, 1787–1799.

22. Nguyen, M.T.; Pignedoli, C.A.; Treier, M.; Fasel, R.; Passerone, D. The Role of Van der Waals Interactions in Surface-Supported Supramolecular Networks. *Phys. Chem. Chem. Phys.* **2010**, *12*, 992–999.

23. Tonigold, K.; Gross, A. Adsorption of Small Aromatic Molecules on the (111) Surfaces of Noble Metals: A Density Functional Theory Study with Semiempirical Corrections for Dispersion Effects. *J. Chem. Phys.* **2010**, *132*, 224701.

24. Wyckoff, R.W.G. *Crystal Structures* (Vol. 1); Interscience Publishers: New York, 1963.